Journal of the Korean Physical Society, Vol. 49, No. 4, October 2006, pp. 1558∼1564

Sub-Bandgap Photonic Base Current Method for Extracting the Trap Density at Heterointerfaces in Heterojunction Bipolar Transistors

S. W. Kim, J. U. Lee, G. C. Kang, K. S. Roh, S. H. Seo,
K. Y. Kim, C. H. Lee, S. Y. Lee, H. T. Kim, D. H. Kim,
K. S. Min, D. J. Kim, D. W. Kang, J. K. Rhee* and D. M. Kim†
School of Electrical Engineering, Kookmin University, Seoul 136-702

(Received 28 March 2006)

We propose a novel photonic base current method to extract the energy-dependent distribution of interface states in heterojunction bipolar transistors (HBTs) by using the photonic current-voltage (I-V) characteristics under sub-bandgap ($E_{ph} < E_g$) photonic excitation. For the sub-bandgap photonic I-V characterization of HBTs, an optical source with a photon energy less than the bandgap energy of $Al_{0.3}Ga_{0.7}As$ and GaAs ($E_{ph} = 0.95$ eV $< E_{g,\mathrm{AlGaAs}} = 1.79$ eV & $E_{g,\mathrm{GaAs}} = 1.42$ eV) is employed for the characterization of interface states distributed over the photo-responsive energy band (E_C –0.95 $\leq E_{it} \leq$ 0.98 eV) at the emitter-base heterojunction in HBTs by comparing the base currents under a dark condition and sub-bandgap photonic excitation. The trap density at the emitter-base heterojunction interface has been obtained as $D_{it} = 10^8 \sim 10^{12}$ eV^{-1}cm^{-2} over the photo-responsive energy band of AlGaAs/GaAs HBTs under sub-bandgap photonic excitation.

PACS numbers: 73.40.-c, 71.55.Eq, 72.40.+w
Keywords: Interface states, Heterojunction, HBT, Sub-bandgap, Photon, Characterization, Bipolar

I. INTRODUCTION

For the purpose of improving speed and high-frequency performance, downscaling of the AlGaAs/GaAs hetero-junction bipolar transistor (HBT) structure has increased the collector current density to the range of 10^5 to 10^6 A/cm^2 under normal bias conditions. This high-current handling capability makes HBTs very attractive for high-power, high frequency microwave amplifier applications [1]. Due to such fast scaling, the thickness of the base layer can be significantly scaled down and various base heterojunction, have been attempted. The base layer is also subject to a high electric field due to the built-in electric field with composition grading and/or doping grading. Therefore, an ultra-thin base layer needs to have very high doping and excellent interface properties. The high doping concentrations in the emitter and base to achieve better current gain with higher cut-off frequency rate already cover the range from 10^{18} to 10^{19} cm^{-3}

In addition, with the development of high-speed digital and mixed analog-digital signal processing circuits and the low-voltage operations, circuit designers require accurate HBT model parameters for circuit simulations. Reliability and performance degradation are also key concerns in the implementation of high-performance HBTs and their integrated circuits as Microwave Monolithic Integrated Circuits and Millimeter-wave Monolithic Integrated Circuits.

The interface traps at the AlGaAs/GaAs interfaces in HBT structures are known to play an important role in determining the 1/f noise, the carrier mobility (μ), the ideality factor (η), the current gain (β), and the base leakage current with degradation of device reliability in HBTs [2–6]. Therefore, accurate modeling and characterization of interface traps throughout the bandgap are the most important topics for improving the robustness of devices and integrated circuits with HBTs. There have been enormous efforts to accurately characterize interface traps in HBTs [7]. The interface traps are the most important characteristic parameters for DC and microwave performance, for noise performances and especially for the reliability of HBTs [8–10].

Photonic characterizations in the previous works used a photon energy (E_{ph}) larger than the bandgap energy. In this work, however, a photon energy smaller than the bandgap energy is used to characterize the interface traps at heterojunction in HBTs. In this work, a new base

*Department of Electronic Engineering and Millimeterwave Innovation Technology (MINT) Research Center, Dongguk University, Seoul 100-715;
†E-mail: dmkim@kookmin.ac.kr; drlife@kookmin.ac.kr;
Tel: +82-2-910-4719; Fax: +82-2-910-4449

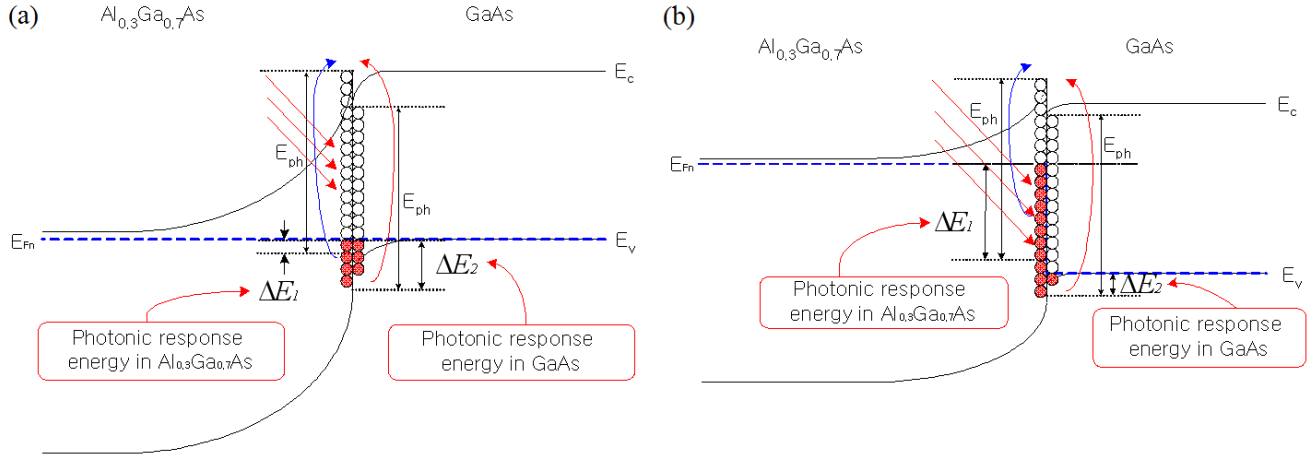

Fig. 1. Schematic energy band diagram of the emitter-base heterojunction in HBTs with optical input (λ = 850 nm; E_{ph} = 1.45 eV > $E_{g,\mathrm{GaAs}}$) : (a) under thermal equilibrium and (b) under forward bias.

current technique, called the 'Photonic Base Current Method (PBCM),' is presented to extract the HBT interface trap density. Based on the photonic high-frequency current-voltage response of photodiode and the emitter-base junction in the HBT, the result of the base current shows extreme peak characteristics with respect to the optical power in the forward bias. Such an abnormal base current normally does not take place over the entire operation region, but rather only in a certain voltage range. There are two kinds of traps, bulk traps and interface traps. In the reverse mode, bulk traps contribute to the abnormal base current. However, in the forward mode, interface traps contribute to the abnormal base current. However, the contribution of the interface traps to the abnormal base current dominate the contribution from bulk traps. In addition, depending on the process in the HBTs, the bias range where the abnormal current occurs may be different. In this way, the difference of the base current under a forward bias directly demonstrates the magnitude of the interface traps. We propose the novel and effective PBCM using the optical current-voltage (I-V) curve as a means of satisfying the above requirement. The basic principle of this method is introduced, and its validity is also verified by the experiments with Npn HBT devices.

II. PHOTONIC I-V CHARACTERISTICS OF AN EMITTER-BASE HETEROJUNCTION

In this section, we describe the photonic current-voltage characteristics of HBTs. Variations of the I-V characteristics of the emitter-base heterojunctions in HBTs are believed to show enough information on the traps and the interface states under a sub-bandgap photonic excitation. Those traps and states is strongly depend on the energy band diagram caused by the applied bias [2].

1. Photonic Base Current Analysis with λ = 850 nm (E_{ph} = 1.45 eV)

In this experiment, we used an optical source with E_{ph} = 1.45 eV (λ = 850 nm) which is larger than the bandgap energy of the GaAs base layer. The band diagrams under thermal equilibrium and forward-bias conditions are illustrated in Figs. 1 (a) and (b), respectively. An optical source with various optical powers (P_{opt} = 0.2 mW, 0.6 mW, and 1.0 mW) was used for the optical excitation of electrons at the interface states in on-wafer HBTs.

Under reverse bias with photonic illumination, photogenerated electrons from the valence band of the emitter-base and the base-collector junctions [band-to-band generation] contribute to the base leakage currents as shown in Fig. 2. However, the numbers of the photogenerated electrons from interface traps and bulk traps are very small compared with that of the photogenerated electrons from the valence band.

The photogenerated electrons from the valence band in the base layer [band-to-band generation] contribute to the base leakage current. The photogenerated electrons from interface traps and bulk traps at the emitter-base layer [trap-to-band generation] also contribute to base leakage current. Under an increase in bias with photonic excitation, the response of the interface traps in the emitter-base heterojunction increases. However, the absolute response is dominated by the excess carriers excited from the band-to-band generation rather than by interface traps [11,12]. Therefore, the use of an optical source with λ = 850 nm isn't appropriate to characterize the interface traps in bipolar junctions.

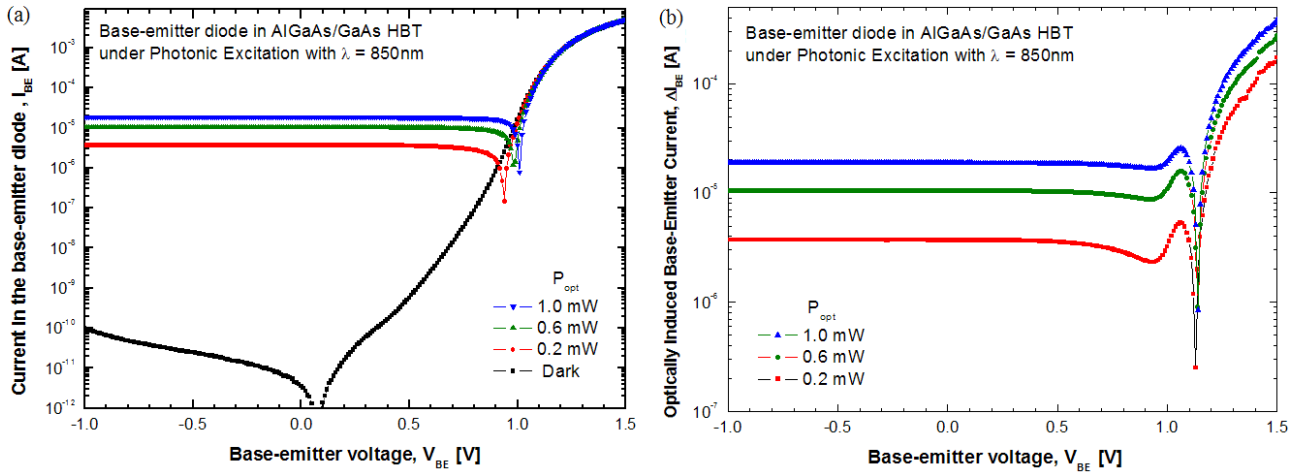

Fig. 2. I-V characteristics of the $Al_{0.3}Ga_{0.7}As$/GaAs HBT under optical illumination (E_{ph} = 1.45 eV, P_{opt} = 0.2, 0.6, 1.0 mW) [band-to-band generation] : (a) DC base-emitter current with photonic illumination and (b) changes of DC base-emitter current with photonic illumination.

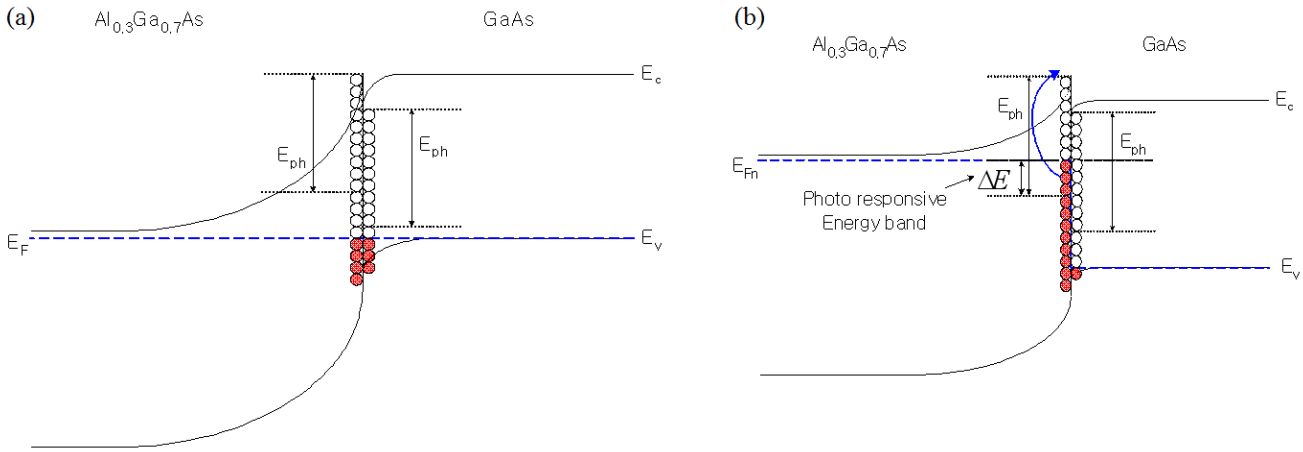

Fig. 3. Energy band diagram of emitter-base heterojunction in HBTs with a sub-bandgap optical input (λ = 1310 nm; E_{ph} = 0.95 eV > $E_{g,\mathrm{GaAs}}$) : (a) under thermal equilibrium and (b) under forward bias.

2. Sub-Bandgap Photonic Base Current Analysis with λ = 1310 nm (E_{ph} = 0.95 eV)

We uses a sub-bandgap photonic source with E_{ph} = 0.95 eV (= 1310 nm), which is smaller than bandgap energy of the GaAs base layer and the wide bandgap $Al_{0.3}Ga_{0.7}As$ emitter layer. The energy band diagrams under thermal equilibrium and forward-bias conditions are illustrated in Figs. 3(a) and (b), respectively. Photogenerated excess electrons from the band-to-band generation in the AlGaAs layer or the GaAs layer do not exist under this sub-bandgap photonic excitation. Under a forward bias condition with sub-bandgap photonic excitation, both bulk traps in the space-charge region at the emitter/base interface and interface traps in the emitter-base heterojunction respond. However, the absolute response is dominated by the excited excess carriers from the interface traps [2,13] not by the band-to-band generation with $E_{ph} < E_g$. An optical source with various optical powers (P_{opt} = 0.2 ∼ 3.0 mW) was used for the sub-bandgap optical excitation and trap characterization in on-wafer HBTs.

The bulk traps located in the space charge regions of the emitter, the base, and the collector contribute to the same extent to the photonic response of HBTs. However, contribution from the bulk traps is negligible because there are few traps in epitaxially-grown bulk layers, and we used sub-bandgap photons having no contribution to the band-to-band excitation of carriers. On the other hand, interface traps located in the emitter-base heterointerface can be major contributors to a change in the photonic current-voltage characteristics in HBTs. Under a forward bias with sub-bandgap photonic excitation, bulk traps in the depletion region at the GaAs/GaAs

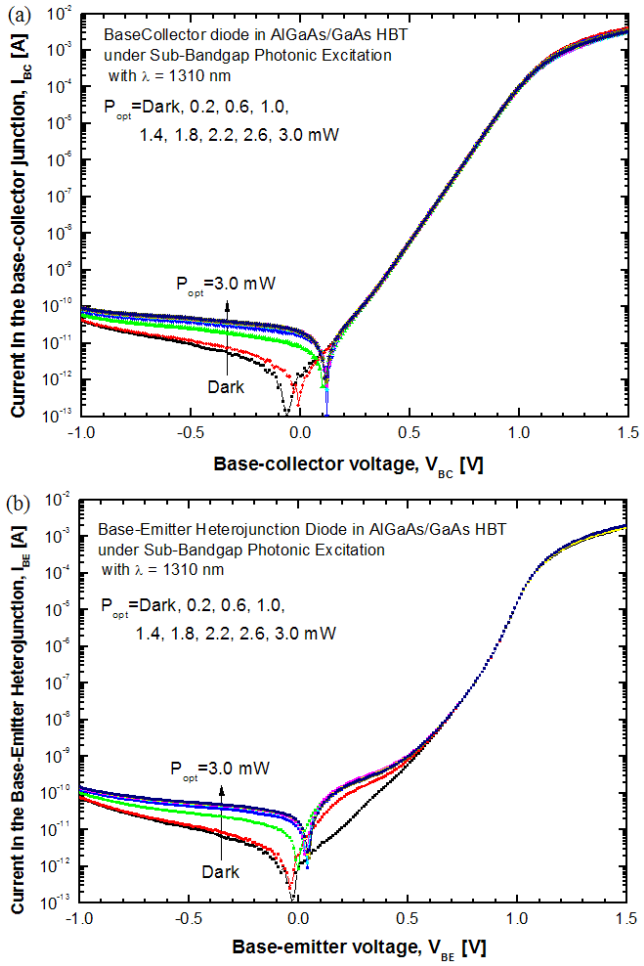

Fig. 4. I-V characteristics of the $Al_{0.3}Ga_{0.7}As/GaAs$ HBT with and without sub-bandgap photonic illumination (E_{ph} = 0.95 eV, $P_{opt} = 0.2 \sim 3$ mW), [trap-to-band generation] : (a) DC base-collector current under photonic illumination and (b) DC base-emitter current under photonic illumination.

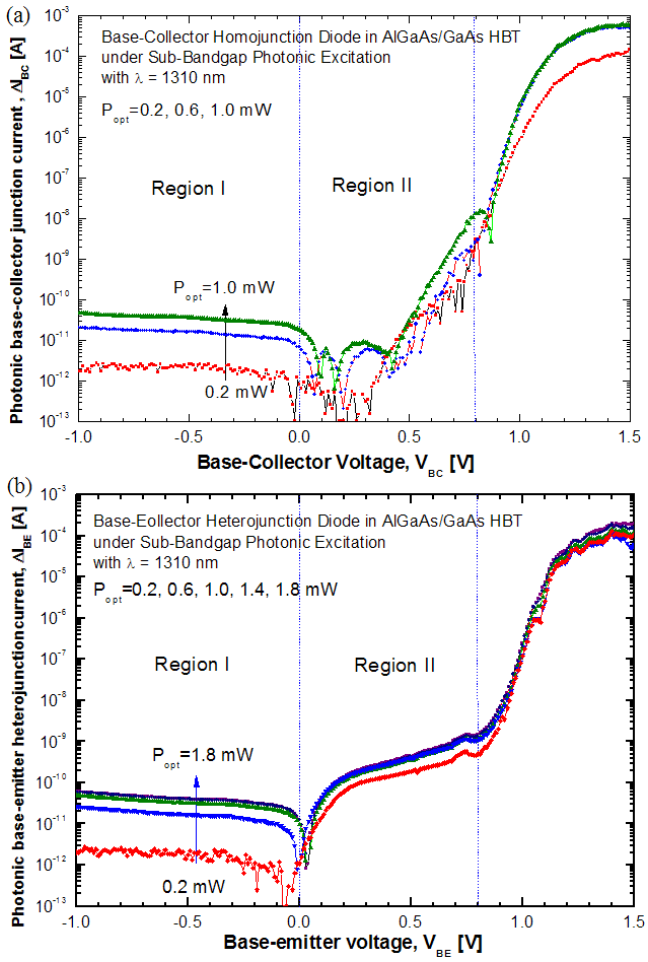

Fig. 5. Optically induced I-V characteristics of the $Al_{0.3}Ga_{0.7}As/GaAs$ HBT (E_{ph} = 0.95 eV, $P_{opt} = 0.2 \sim 1.8$ mW) [trap-to-band generation] : (a) base-collector junction and (b) base-emitter junction.

base-collector layer responded to the photonic energy as shown in Fig. 4 (a), and both bulk traps and interface traps in the depletion region at the $Al_{0.3}Ga_{0.7}As/GaAs$ emitter-base heterojunction responded to the optical energy as shown in Fig. 4 (b). However, the overall response under sub-bandgap photonic excitation was controlled by using the excess carriers generated from the interface traps rather than by using those from bulk.

The increased forward bias moves the Fermi energy level closer to the conduction band. Thus, the number of the photogenerated electrons increases. Therefore, the photonic base current under sub-bandgap photonic excitation increases with increasing base-emitter voltage across the heterojunction, as shown in Fig. 4(b).

In region I of Fig. 5 with a reverse bias under photonic illumination, the photogenerated electrons from the emitter-base and the base-collector regions are closely associated with bulk traps and result in an increased base leakage current. In region II, a considerable difference between the emitter-base and base-collector current is observed. This is due to the photogenerated excitation of carriers throughout the interface traps in the N-$Al_{0.3}Ga_{0.7}As$/p-GaAs emitter-base heterojunction rather than in the p-GaAs/n-GaAs base-collector homojunction.

III. SUB-BANDGAP PHOTONIC BASE CURRENT METHOD AND EXPERIMENTAL RESULT

We describe the used device, the measurement setup, the modeling of interface recombination current, and the experimental observation. A schematic of the cross-sectional structure of the gas-source MBE-grown AlGaAs/GaAs HBT is shown in Fig. 6, and a simplified structure is shown in Fig. 7. The emitter/base junction is a heterojunction ($Al_{0.3}Ga_{0.7}As/GaAs$)

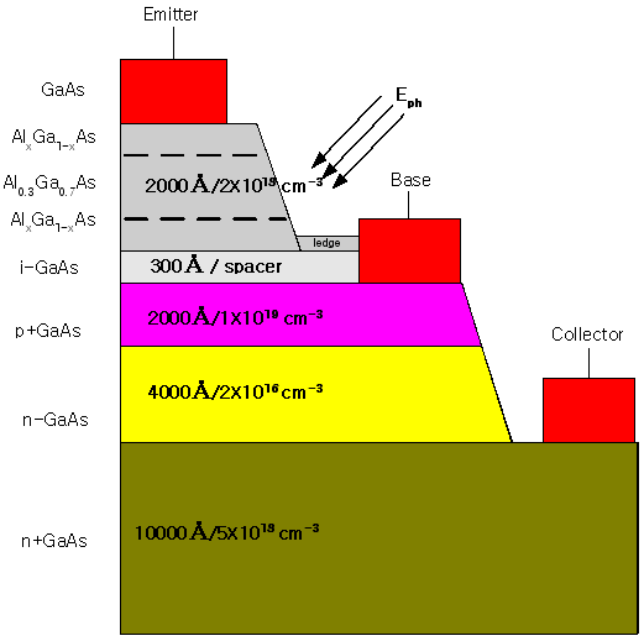

Fig. 6. Cross-sectional structure of characterized AlGaAs/GaAs HBTs.

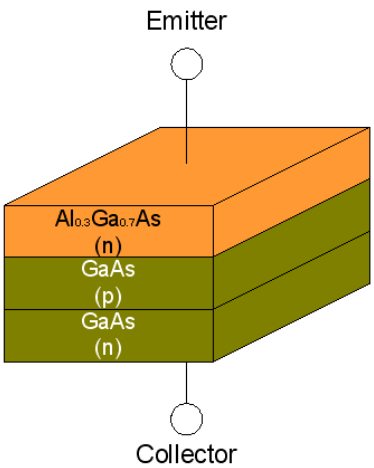

Fig. 7. Simplified device cross-section of characterized AlGaAs/GaAs HBTs.

and the base/collector junction is a homojunction (GaAs/GaAs). Thus, a lattice mismatch occurs at the $Al_{0.3}Ga_{0.7}As$/GaAs emitter-base heterointerface. The heterojunction has more interface traps than the homojunction due to the lattice mismatch. The measured device has good electrical characteristics under dark conditions as shown in Fig. 8. The optically excited electrical characteristics of an emitter-base junction in HBT with $W_E \times L_E = 250 \times 100\ \mu m^2$ were measured with an optical source (λ = 1310 nm ; ILX Lightwave Co Model 7200), a Cascade probe station, and an HP4145B semiconductor parameter analyzer as shown in Fig. 9.

We investigated variations of the current-voltage characteristics of the HBTs and investigated the interface traps by comparing the dark current with the photonic diode current under sub-bandgap photonic excitation. An increased forward bias moves the Fermi energy level

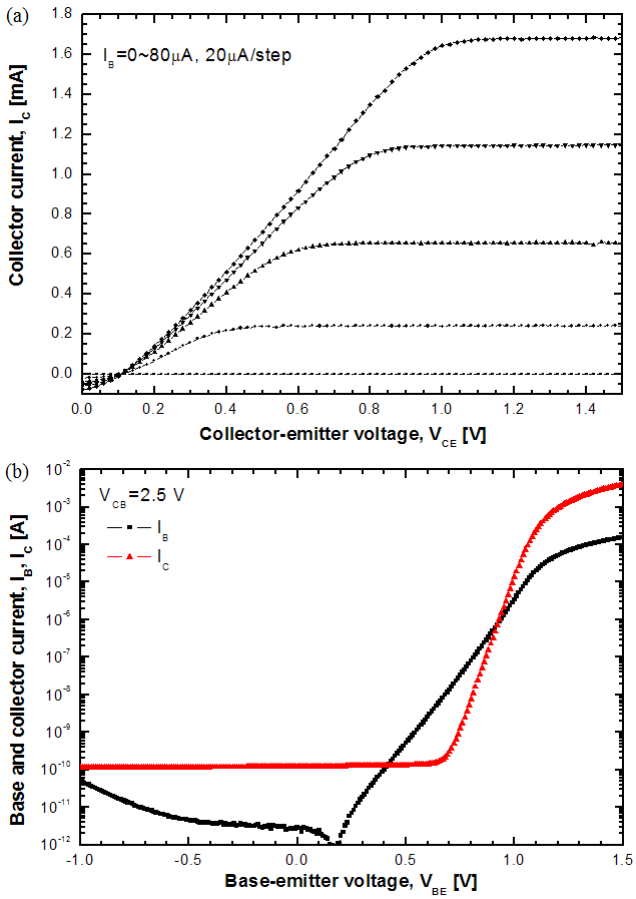

Fig. 8. I-V characteristics of an HBT with emitter-base junction area of $W_E = 250\ \mu m$ by $L_E = 100\ \mu m$.

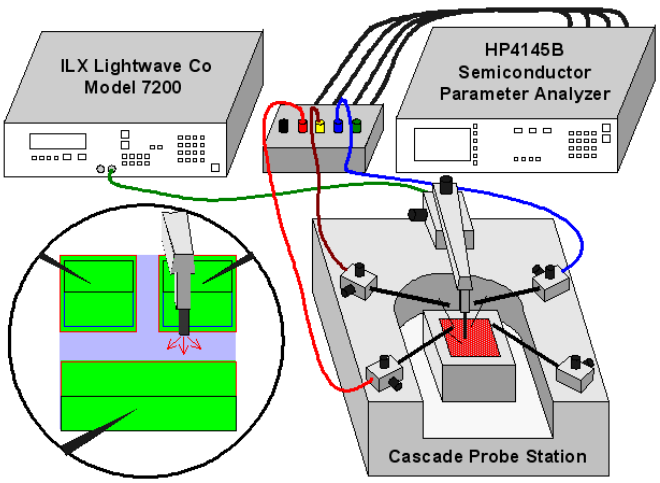

Fig. 9. Experimental setup of the PBCM method for characterizing the interface states in HBTs.

closer to the conduction band. Therefore, the number of photogenerated electrons increases. Therefore, the photonic base current under sub-bandgap photonic excitation increases with increasing base-emitter voltage across the heterojunction, as shown in Fig. 4 (b).

In region II, a considerable difference between the emitter-base current and the base-collector current is observed. This is due to photogenerated electrons throughout the interface traps in the emitter-base heterojunction rather than to those throughout the interface traps in the base-collector homojunction. In this case, the Shockley-Read-Hall (SRH) recombination rate R_{SRH} is increased because of the excess carriers under sub-bandgap photonic illumination. The recombination rate due to the SRH recombination mechanism is given by [14,15]

$$R_{SRH} = \frac{np - n_i^2}{\tau_{po}(n + n') + \tau_{no}(p + p')}, \quad (1)$$

where n_i is the intrinsic carrier concentration, $n(p)$ is the electron (hole) concentration, $n'(p')$ is the electron (hole) density in the traps, and $\tau_{no}(\tau_{po})$ is the electron (hole) lifetime.

When a sub-bandgap optical excitation is applied to the HBT being characterized, R_{SRH} is changed into $R_{SRH} + \Delta R_{SRH}$ as a result of the trap-to-band generated excess carriers. The number of excess carriers is proportional to the interface trap density in the photoresponsive energy band in the forbidden energy band ($E_V < E < E_C$). The optically induced recombination rate (ΔR_{SRH}) can be expressed as

$$\Delta R_{SRH} = R_{SRH,optical} - R_{SRH,dark}, \quad (2)$$

where $R_{SRH,optical}$ is the recombination rate under sub-bandgap photonic illumination while $R_{SRH,dark}$ is the recombination rate under dark conditions. The optically-induced base current $\Delta I_{BE.rec}$ is calculated from

$$\Delta I_{BE.rec} = qA_E \int_{-x_n}^{x_p} \Delta R_{SRH} dx, \quad (3)$$

where x_p and x_n are the depletion widths of the p-type base and the n-type emitter, respectively. The measured $\Delta I_{BE,rec}$ is plotted in the region II of Fig. 5(b).

The photogenerated electrons from the interface traps in the emitter-base heterojunction generation under sub-bandgap photonic excitation are dominant over those from bulk traps because there is no band-to-band generation without traps in the forbidden band. The optically induced base current can be modeled by [16]

$$\Delta I_{BE.rec} = qA_E \int_{N_{it}} \Delta R_{SRH,it} dx, \\ = \frac{1}{2} qA_E \sigma v_{th} \Delta N_{it} n_{iB} \exp\left(\frac{V_{BE}}{2V_{th}}\right), \quad (4)$$

where $\Delta R_{SRH,it}$ is the SRH recombination rate through the interface states, σ is the capture cross-section, v_{th} is the thermal velocity, N_{it} is the number of interface traps,

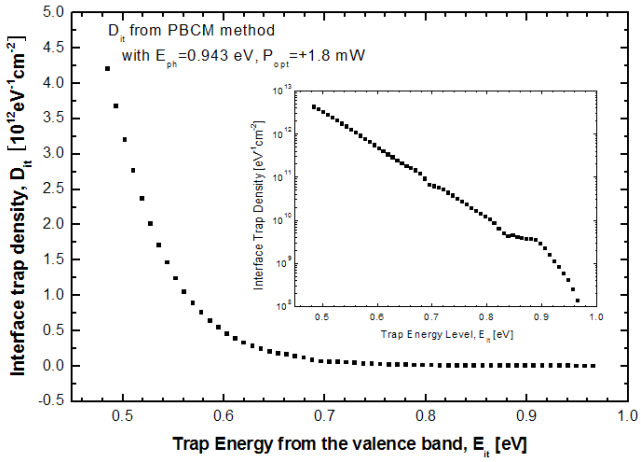

Fig. 10. D_{it} extracted from the $Al_{0.3}Ga_{0.7}As/GaAs$ emitter-base heterointerface.

n_{iB} is the intrinsic carrier concentration in the GaAs base region, and V_{th} is the thermal voltage. Therefore, the interface trap density D_{it} can be finally obtained from

$$D_{it} = \frac{\partial \Delta N_{it}}{\partial E} \\ = \frac{\partial}{\partial E}\left[\frac{2\Delta I_{BE.rec}}{qA_E \sigma v_{th} n_{iB}} \exp\left(-\frac{V_{BE}}{2V_{th}}\right)\right]. \quad (5)$$

We applied the proposed PBCM method to HBTs with an emitter area $A_E = W_E \times L_E = 250 \times 100\ \mu m^2$, which were fabricated by using the conventional mesa process ($N_{DE} = 2 \times 10^{18}$ cm^{-3}, $N_{AB} = 1 \times 10^{19}$ cm^{-3}, $\sigma \sim 10^{-14}$ cm^2, $v_{th} \sim 10^7$ cm/s, $n_{iB} = 1.8 \times 10^6$ cm^{-3}). We comparatively investigated the variations in the current-voltage characteristics of HBTs and extracted the number of interface traps by comparing the emitter-base currents under dark conditions with the current under sub-bandgap photonic excitation. A sub-bandgap optical source with $\lambda = 1310$ nm ($E_{ph} = 0.95$ eV) and with various optical powers ($P_{opt} = 0.2 \sim 3.0$ mW) was used for the trap characterization in on-wafer HBTs. However, the number of traps reactions due to sub-bandgap photonic excitation was saturated for $P_{opt} > 1.8$ mW, as shown in Fig. 5(b). Comparing the base current of the emitter-base junction under $E_{ph} < E_g$ with $P_{opt} = 0$ and 1.8 mW, we obtained the energy dependent distribution of D_{it} over the photoresponsive energy band (E_C –0.95 $\leq E_{it} \leq$ 0.98 eV) at the emitter-base heterointerfaces in AlGaAs/GaAs HBTs. The extracted trap density at the $Al_{0.3}Ga_{0.7}As/GaAs$ emitter-base heterointerface is shown in Fig. 10. The trap density at the emitter-base heterojunction interface was obtained as $D_{it} = 10^8 \sim 10^{12}$ eV^{-1}cm^{-2} over the photoresponsive energy band for AlGaAs/GaAs HBTs under sub-bandgap photonic excitation.

IV. CONCLUSION

Sub-bandgap photonic excitation $E_{ph} < E_g$ was used to extract of the interface trap density at the $Al_{0.3}Ga_{0.7}As/GaAs$ emitter-base heterointerfaces of HBTs by using a new photonic base current method (PBCM) for the first time. By comparative probing of the base currents with and without sub-bandgap photonic excitation, we could extract the interface trap density from the experimental data. The data extracted by using the PBCM gave $D_{it} = 10^8 \sim 10^{12}$ $eV^{-1}cm^{-2}$. The validity of this technique was qualitatively explained by using the data measured from the base-emitter leakage currents with and without sub-bandgap photonic excitation.

ACKNOWLEDGMENTS

This work was supported by 2006 Kookmin University Research Initiative.

REFERENCES

[1] A. Sanseverino and P. Spirito, 50th European Conference on Power Electronics and Appl. **2**, 58 (1993).
[2] H. T. Shin, K. H. Kim, K. S. Kim, I. C. Nam, J. B. Choi, J. U. Lee, S. W. Kim, H. T. Kim, T. E. Kim, H. S. Park, G. C. Kang, D. J. Kim, K. S. Min, D. W. Kang and D. M. Kim, J. Korean Phys. Soc. **44**, 1485 (2004).
[3] B. R. Ryum and I. M. Abdel-Motaleb, in IEE Proceedings of Circuits, Devices and Systems **138**, 115 (1991).
[4] R. E. Welser, N. Pan, Vu Duy-Phach, P. J. Zampardi and B. T. McDermott, IEEE Trans. Electron Dev. **46**, 1599 (1999).
[5] J. Kang, K. Lee, D. Yu and B. Kim, J. Korean Phys. Soc. **41**, 539 (2002).
[6] A. K. Kirtania, M. B. Das, S. Chandrasekhar, L. M. Lunardi, G. J. Qua, R. A. Hamm and L.-W. Yang, IEEE Trans. Electron Dev. **43**, 784 (1996).
[7] J.-M. Lee, B.-G. Min, S.-I. Kim, K.-H. Lee and S. H. Park, J. Korean Phys. Soc. **40**, 320 (2002).
[8] G. Niu, J. D. Cressler and A. J. Joseph, IEEE Trans. Electron Dev. **45**, 2499 (1998).
[9] J. J. Liou, *CAS '98 Proceedings of International Semiconductor Conference* 23 (1998).
[10] T. Henderson, in *Proceedings of GaAs Reliability Work shop* 181 (2001).
[11] C. K. Song, S. H. Lee and K. D. Kim, IEEE Electron Dev. Lett. **22**, 315 (2001).
[12] Z. H. Lu, A. Majerfeld, P. D. Wright and L. W. Yang, IEEE Selected Topics in Quantum Elect. **1**, 1030 (1995).
[13] T. E. Kim, H. T. Kim, H. T. Shin, H. S. Park, K. S. Kim, I. C. Nam, K. H. Kim, J. B. Choi, J. U. Lee, S. W. Kim, G. C. Kang, D. J. Kim, K. S. Min, D. W. Kang and D. M. Kim, J. Korean Phys. Soc. **44**, 1479 (2004).
[14] W. Liu, *Handbook of III-V Heterojunction Bipolar Transistors* (John Wiley & Sons, New York, 1998), p. 117.
[15] D. A. Neamen, *Semiconductor Physics and Devices: Basic Principles* (Irwin, Chicago, 1997), p. 266.
[16] J. J. Liou, IEEE Trans. Electron Dev. **36**, 1850 (1989).